# Chemical Science

Accepted Manuscript


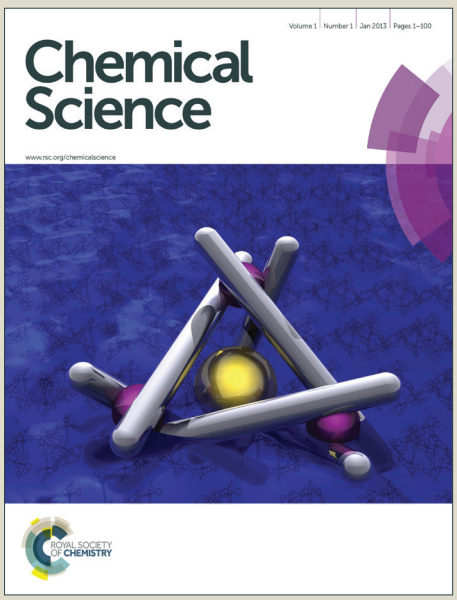





ROYAL SOCIETY OF CHEMISTRY

www.rsc.org/chemicalscience

Chemical Science

RSCPublishing

ARTICLE

# Biosynthesis of trioxacarcin revealing a different starter unit and complex tailoring steps for type II polyketide synthase†

Cite this: DOI: 10.1039/xoxxoooooox

Received 12th January 2015,
Accepted ooth January 2015

DOI: 10.1039/xoxxoooooox

www.rsc.org/chemicalscience

Mei Zhang,‡[a] Xian-Feng Hou,‡[a] Li-Hua Qi,[a] Yue Yin,[a] Qing Li,[a] Hai-Xue Pan,[a] Xin-Ya Chen[a] and Gong-Li Tang*[ab]

Trioxacarcins (TXNs) are highly oxygenated, polycyclic aromatic natural products with remarkably biological activity and structural complexity. Evidences from $^{13}$C-labelled precursors feeding studies demonstrated that the scaffold was biosynthesized from one unit of *L*-isoleucine and nine units of malonyl-CoA, which suggested a different starter unit in the biosynthesis. Genetic analysis of the biosynthetic gene cluster revealed 56 genes encoding a type II polyketide synthase (PKS) combining with a large amount of tailoring enzymes. Inactivation of seven post-PKS modification enzymes resulted in the production of a series of new TXN analogues, intermediates, and shunt products, most of which show high anticancer activity. Structural elucidations of these new compounds not only help us to propose the biosynthetic pathway featuring a type II PKS using a novel starter unit, but also set the stage for further characterization of the enzymatic reactions and combinatorial biosynthesis.

## Introduction

Microorganisms could produce a large variety of biologically active secondary metabolites representing a vast diversity of fascinating molecular architecture, which usually spurs particular attentions for chemical synthesis, mode of action, biosynthesis, and even drug discovery. As one of examples, trioxacarcin A (TXN-A, **1**, Fig. 1) represents a special family of complex aromatic natural products which was first isolated from *Streptomyces bottropensis* DO-45 (NRRL 12051) in 1981,[1-3] and subsequently re-isolated from a marine *Streptomyces* sp. B8652 with a series of analogues in 2004.[4,5] It displays extraordinary anti-bacterial, anti-malaria, and anti-tumor activity with subnanomolar $IC_{70}$ values in various cancer cell lines.[1-5] Structurally, TXN-A contains unusual condensed polycyclic trisketal bearing a fused spiro-epoxide, which is believed as a "warhead" to covalently bound to DNA, followed by cleavage of the resultant TXN-DNA complexes and yielded another natural product gutingimycin (**3**, Fig. 1) through an abstraction of the guanine.[6,7] In addition, it has unique glycosylation patterns including a rare γ-branched octose.

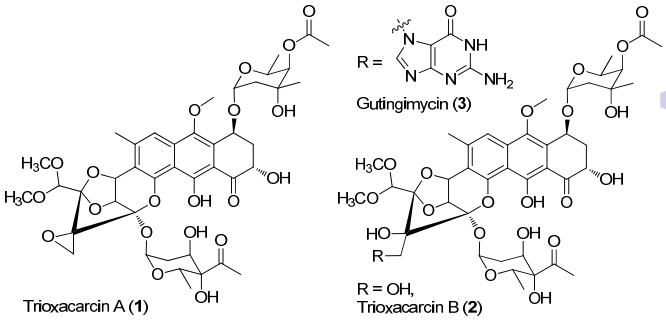


**Fig. 1** Chemical structure of trioxacarcin (TXN) and relative natural products.

The high biological activities, especial anticancer activity, along with unusual and complex structural features of TXN-A distinguish it from other aromatic polyketides, thus leave an interesting but challenging target to the total synthesis. Until recently, Myers's group successfully established a multiply convergent, component-based route to chemically synthesize TXN-A and its structural analogues.[8,9] However, the biosynthetic studies have never been explored to these structurally complex antibiotics. Herein, we describe 1) the incorporation studies with the $^{13}$C-labeling precursors, which elucidated the biosynthetic origin of the scaffold for the TXN family of natural products; 2) the genetic characterization of *txn* gene cluster, which afforded four polyketide derivates and seven TXN analogues; and 3) a proposed biosynthetic pathway, which involving a different starter unit for priming type II polyketide synthase (PKS) and complex tailoring steps.

[a]*State Key Laboratory of Bio-organic and Natural Products Chemistry, Shanghai Institute of Organic Chemistry, Chinese Academy of Sciences, 345 Lingling Road, Shanghai 200032, China. E-mail: gltang@sioc.ac.cn*

[b]*Shanghai Collaborative Innovation Center for Biomanufacturing Technology, 130 Meilong Road, Shanghai 200237, China*

† Electronic Supplementary Information (ESI) available: The experimental procedures, strains, plasmids and PCR primers, and compound characterization. See DOI:10.1039/b000000x/

‡ M. Zhang and X.-F. Hou contributed equally to this work.

## Results and discussion

### Biosynthetic origin of the polycyclic scaffold of TXNs

TXN-A was originally reported from *S. bottropensis* DO-45 with the isolation of 20 mg from a 18 L of fermentation broth,[1,2] this titer is not efficient enough for the biosynthetic studies. In our early effort to optimize the fermentation and isolation processes, we noticed that the yield of TXN-A could be significantly improved by hundred times through addition of hydrophobic resin HP-20 into the fermentation medium, even up to titers of 100-200 mg/L in shaking flasks.[10] Under this optimized condition, the precursors [1-$^{13}$C]-acetate, [2-$^{13}$C]-acetate, and [1,2-$^{13}$C]-acetate were added into a fermentation culture (a total of 0.7 g/L) by pulse feeding after 48, 56, 64, 72, 80, 88 hr of incubation in separate incorporation experiments, and the fermentation was lasted to 120 hr. TXN-A isolated from the feeding fermentations was subjected to $^{13}$C-NMR analysis to confirm the polyketide extender units of the scaffold (ESI, Table S1). All the $^{13}$C abundance at each positions of the TXN-A backbone could be sufficiently separated and identified (ESI, Fig. S1). Thus, the incorporation results were summarized in Table S1 and Fig. 2A. Significant enrichments were observed at C-1, C-3, C-4a, C-6, C-8, C-9, C-10a, and C-11 in [1-$^{13}$C]-acetate labelled TXN-A, as well as C-2, C-4, C-5, C-7, C-8a, C-9a, C-10, C-12, and C-18 in [2-$^{13}$C]-acetate labelled TXN-A both suggested the folding pattern of polyketide chain in Fig. 2A, which was further supported by [1,2-$^{13}$C]-acetate feeding results (Fig. S1 and Table S1). Obviously, the right ring contains three malonate-derived intact acetate units (C-9a to C-1, C-2 to C-3, and C-4 to C-4a), which suggested the folding pattern of the polyketide chain could be classified into typical streptomyces mode.[11] In addition, the incorporation of [2-$^{13}$C]-acetate into C-18 indicated a decarboxylation step should be involved in the formation of fused-ring skeleton. However, the labelled pattern of the five-carbon (C-13, C-14, C-15, C-16, and C-17) remains confused, which hints that this five-carbon unit may be derived from other origin. Moreover, the five-carbon unit was likely employed by the type II PKS as a non-acetate starter unit to generate the polyketide in which the decarboxylation is usually performed on the last carbon of the fully elongated polyketide chain.

A five-carbon unit (C-13 to C-17), most possibly from 2-methylbutyryl-CoA, serving as the starter unit of PKS was seldom observed in the natural product biosynthesis. The only exception is involved in the biosynthesis of avermectin "a" components, which are 16-membered macrocyclic lactones generated by type I PKS through loading 2-methylbutyryl-CoA as the starter unit.[12] For the type II PKS, although non-acetate starter units, including propionate, malonamate, polyketide or fatty acid, and even amino acid derivates have also been employed,[13] 2-methylbutyryl-CoA has never been reported as starter unit to generate aromatic polyketides. Given the fact that 2-methylbutyryl-CoA is usually derived from *L*-isoleucine (Ile) through deamination and deacrboxylation by transaminase and branched-chain 2-oxo acid dehydrogenase *in vivo*, we performed the feeding experiment with $^{13}C_6$-*L*-Ile to validate this hypothesis (Fig. 2A). Remarkably, ESI-MS showed TXN-A from this feeding experiment was +5 *m*/*z* heavier than that without feeding (Fig. 2B), indicating the incorporation of a five-carbon unit which arose from an intact Ile. Further specific and significant signal enrichment at C-13 to C-17 (Fig. 2C) in $^{13}$C-NMR spectra, and all the $^{13}$C–$^{13}$C coupling data (Fig. 2D) are well consistent with the same conclusion ($J_{C\text{-}16/C\text{-}15}$ = 62 Hz, $J_{C\text{-}15/C\text{-}14}$ = 58 Hz, $J_{C\text{-}13/C\text{-}14}$ = 54 Hz, and $J_{C\text{-}17/C\text{-}14}$ = 32 Hz), which are agreement with that this five-carbon unit originated from Ile via an intact incorporation manner. Thus, these results unambiguously demonstrated that the missing five-carbon unit, C-13 to C-17, is derived from *L*-Ile, which most likely following deamination and deacrboxylation process similar to that of avermectin "a" components biosynthesis.[12]

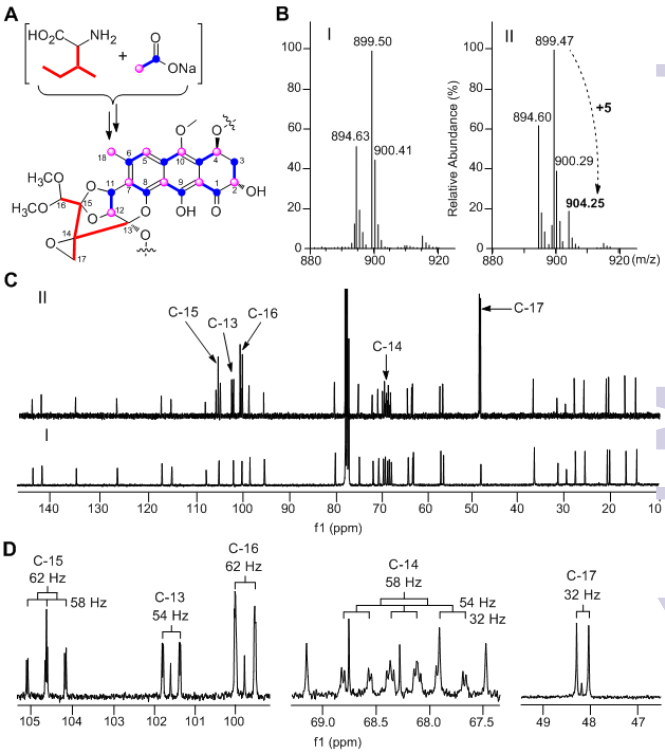


**Fig. 2** Characterization of the biosynthetic origin of TXNs by precursor feeding experiments. (A) Summary of feeding results with $^{13}$C-labeled sodium acetate and $^{13}C_6$-*L*-isoleucine (Ile). (B) MS analysis of production of TXN by fermentation without (I) or with $^{13}C_6$-*L*-Ile (II). (C) $^{13}$C-NMR spectra of TXN-A with (II) and without (I) feeding of $^{13}C_6$-*L*-Ile. The enhanced signals of C-13, C-14, C15, C-16, and C-17 are marked. (D) The enlarged parts of $^{13}$C-NMR spectra from feeding experiment.

### Cloning, sequencing, and identification of the biosynthetic gene cluster of TXNs

The aromatic polycyclic skeleton of TXNs and the primary $^{13}$C-labeled acetate feeding experiments suggest that a type-II PKS should be involved in the biosynthesis. Therefore, we cloned the gene cluster by the PCR approach specific for accessing the genes encoding a ketosynthase (KS)-chain length factor (CLF) heterodimer.[14] By screening of the genomic library and the subsequent chromosome walking, a 102 kb contiguous DNA sequence was mapped into three overlapping fosmids (pTG5001, pTG5002 and pTG5003, Fig. 3A). Sequencing and bioinformatic analysis of these fosmids revealed 91 ORFs, most of which (the *txn* gene cluster) are deposited in GenBank under the accession No. KP410250.

To verify that the cloned gene cluster was involved in TXNs biosynthesis, we constructed a mutant strain TG5001 in which the *txn*A1 gene encoding KS was inactivated by gene disruption (ESI, Fig. S2). As expected, this mutant strain completely abolished the production of TXN-A (Fig. 4A-II), which proved the essential role of this gene cluster governing TXN biosynthesis. Next inactivation of the genes *orf-2* (acyltransferase), *orf-1* (unknown), *orf+11* (cytochrome P450),

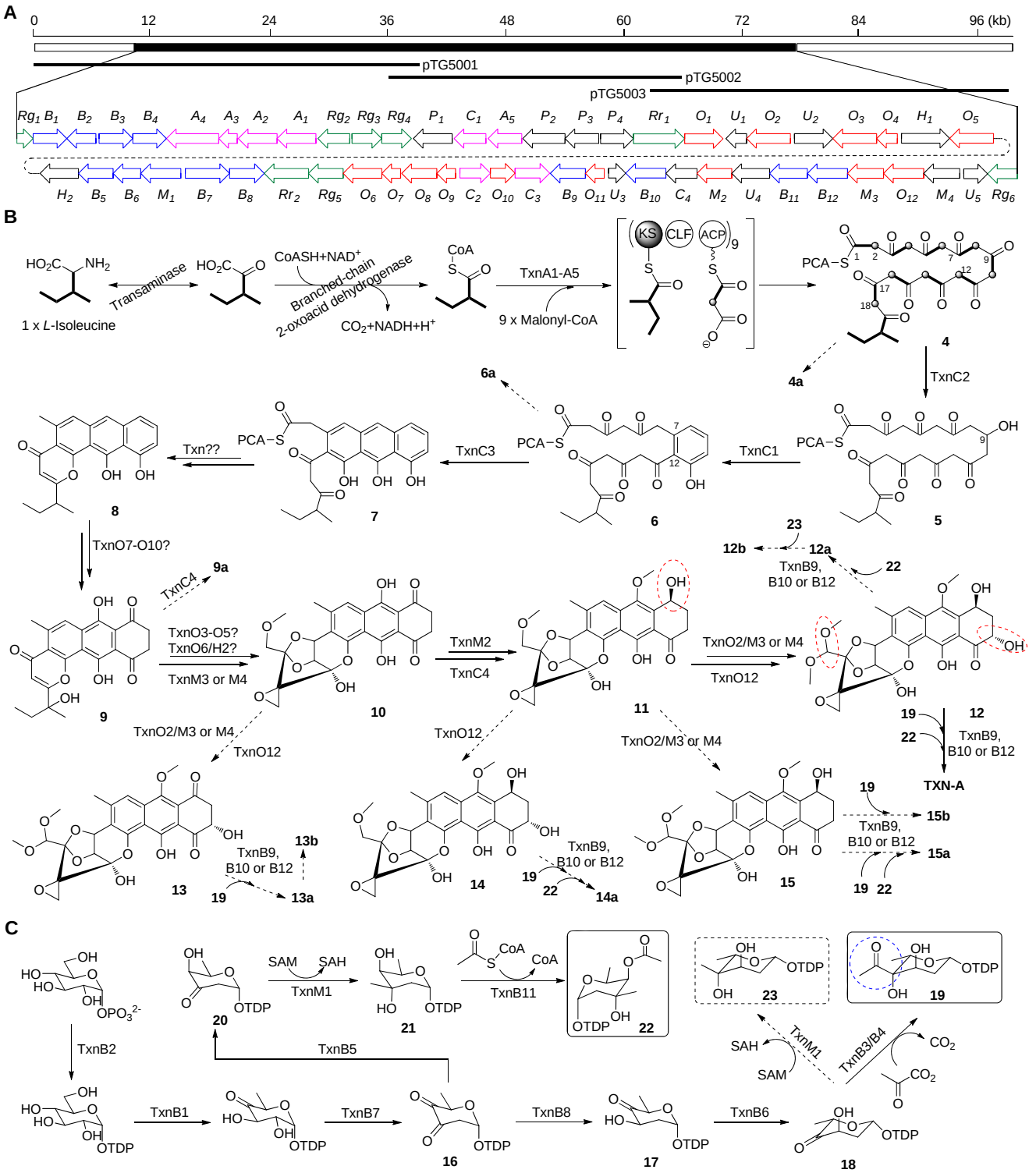


**Fig. 3** Biosynthetic gene cluster and proposed biosynthetic pathway of TXN-A and relative metabolites. (A) Localization of the cloned DNA region as represented by three overlapping fosmids and organization of *txn* gene cluster. Color coding indicates the genes for the PKS and PKS associated enzymes (pink), tailoring enzymes (red), deoxy sugar (blue), regulators and resistant proteins (green), and all others (black). (B) Proposed model for type II PKS and post-PKS modification. (C) Proposed biosynthetic pathway of two deoxysugar moieties. The significant points of the pathway were highlighted by colorful circles.

and *orf+3* (tRNA-synthetase) had no effect on TXN-A production; whereas, inactivation of *txn*Rg1 (regulator) or *txn*Rg6 (regulator) led to obviously decreased the yield of TXN-A (Fig. 4A-III to VIII), which suggested that the *txn* gene cluster may range from *txn*Rg1 to *txn*Rg6, encompassing 56 ORFs (Fig. 3A and Table 1).

**Table 1** Deduced functions of ORFs in *txn* biosynthetic gene cluster

| Gene | AA[a] | Protein homolog (accession no.), origin | S/I[b](%) | Proposed function |
|---|---|---|---|---|
| *txnRg1* | 94 | LuxR family regulator (016578673), *S. albulus* | 65/55 | Regulator |
| *txnB1* | 330 | ChlC2 (AAZ77689), *S. antibioticus* | 76/67 | dTDP-glucose 4,6-dehydratase |
| *txnB2* | 290 | AclY (BAB72036), *S. galilaeus* | 86/74 | dTDP-glucose synthase |
| *txnB3* | 327 | KstD7 (AFJ52686), *Micromonospora* sp. TP-A0468 | 76/66 | Pyruvate dehydrogenase-α |
| *txnB4* | 345 | KstD8 (AFJ52687), *Micromonospora* sp. TP-A0468 | 86/79 | Pyruvate dehydrogenase-β |
| *txnA4* | 561 | OxyP (AAZ78339), *S. rimosus* | 64/53 | MAT |
| *txnA3* | 90 | SsfC (ADE34520), *S.* sp. SF2575 | 76/53 | ACP |
| *txnA2* | 406 | Snoa2 (CAA12018), *S. nogalater* | 77/66 | CLF ($KS_\beta$) |
| *txnA1* | 420 | PgaA (AAK57525), *S.* sp. PGA64 | 84/72 | $KS_\alpha$ |
| *txnRg2* | 263 | DnrI (EFL25867), *S. himastatinicus* ATCC 53653 | 78/63 | SARP-family regulator |
| *txnRg3* | 394 | 2-component kinase (ADO32765), *S. vietnamensis* | 54/40 | 2-component kinase |
| *txnRg4* | 203 | 2-component regulator (CAA09631), *S. violaceoruber* | 82/69 | 2-component regulator |
| *txnP1* | 579 | RkA (ACZ65474), *S.* sp. 88-682 | 57/43 | ATP-dependent CoA synthetase |
| *txnC1* | 318 | ORF27 (AEM44304), e-DNA | 64/50 | Aromatase |
| *txnA5* | 344 | CosE (ABC00733), *S. olindensis* | 70/58 | KS-III |
| *txnP2* | 543 | 2-isopropylmalate synthase (ACY99077), *Thermomonospora curvata* DSM 43183 | 70/58 | 2-isopropylmalate synthase |
| *txnP3* | 417 | Acyl-CoA transferase/dehydratase (EIE99664), *S. glauca* K62 | 67/56 | Dehydratase or isomerase |
| *txnP4* | 260 | Ketoreductase (EDY66493), *S. pristinaespiralis* ATCC 25486 | 63/46 | Short-chain dehydrogenase |
| *txnRr1* | 500 | Actinorhodin transporter (EFL40860), *S. griseoflavus* Tu4000 | 64/48 | Transporter |
| *txnO1* | 345 | Dehydrogenase (ACZ83978), *Streptosporangium roseum* DSM43021 | 74/61 | Dehydrogenase |
| *txnU1* | 126 | Tcur_2795 (ACY98340), *Thermomonospora curvata* DSM 43183 | 40/33 | Unknown |
| *txnO2* | 401 | P450 (CBX53644), *S. platensis* | 66/52 | Cytochrome P450 |
| *txnU2* | 366 | O3I_28241 (EHY24336), *Nocardia brasiliensis* ATCC 700358 | 69/53 | Unknown |
| *txnO3* | 411 | ThcD (AAC45752), *Rhodococcus erythropolis* | 62/48 | Ferredoxin reductase |
| *txnO4* | 107 | 2Fe-2S ferredoxin (ZP_09514545), *Oceanicola* sp. S124 | 68/52 | Ferredoxin |
| *txnH1* | 494 | Putative tripeptidylaminopeptidase (AAP85358), *S. griseoruber* | 68/59 | Hydrolase |
| *txnO5* | 409 | Orf29 (AAP85338), *S. griseoruber* | 68/53 | Cytochrome P450 |
| *txnH2* | 373 | Microsomal epoxide hydrolase (EHI80707), *Frankia* sp. CN3 | 68/56 | Epoxide hydrolase |
| *txnB5* | 328 | PokS9 (ACN64856), *S. diastatochromogenes* | 70/60 | dNDP-hexose-4-ketoreductase |
| *txnB6* | 213 | PokS7 (ACN64855), *S. diastatochromogenes* | 82/72 | 3,5-Epimerase |
| *txnM1* | 413 | TylCIII (AAD41823), *S. fradiae* | 84/73 | dNDP-hexose 3-C-MT |
| *txnB7* | 488 | SaqS (ACP19377), *Micromonospora* sp. Tu 6368 | 71/62 | dNDP-hexose 2,3-dehydratase |
| *txnB8* | 321 | SaqT (ACP19378), *Micromonospora* sp. Tu 6368 | 70/62 | dNDP-hexose 3-ketoreductase |
| *txnRr2* | 500 | EmrB/QacA (EGE43895), *S. griseus* XylebKG1 | 75/59 | Transporter |
| *txnRg5* | 339 | DeoR regulator (ACZ87003), *Streptosporangium roseum* DSM43021 | 77/70 | Regulator |
| *txnO6* | 406 | ORF 3 (AAD28449), *S. lavendulae* | 63/45 | Cytochrome P450 |
| *txnO7* | 175 | PokC1 (ACN64848), *S. diastatochromogenes* | 45/35 | Cyclase or hydroxylase |
| *txnO8* | 371 | AlnT (ACI88867), *S.* sp. CM020 | 57/43 | Hydroxylase |
| *txnO9* | 154 | CalC (AAM70338), *Micromonospora echinospora* | 50/36 | Cyclase or hydroxylase |
| *txnC2* | 261 | HedA (AAP85364), *S. griseoruber* | 83/71 | Ketoreductase |
| *txnO10* | 178 | AsuE2 (ADI58638), *S. nodosus* subsp. *asukaensis* | 57/43 | Flavin reductase |
| *txnC3* | 304 | Gra-ORF33 (ADO32793), *S.vietnamensis* | 68/56 | 2,3-Cyclase |
| *txnB9* | 383 | SsfS6 (ADE34512), *S.* sp. SF2575 | 55/38 | Glycosyl transferase |
| *txnO11* | 148 | Aln2 (ACI88858), *S.* sp. CM020 | 52/41 | Cyclase or hydroxylase |
| *txnU3* | 121 | GrhI (AAM33661), *S.* sp. JP95 | 46/28 | Unknown |
| *txnB10* | 424 | UrdGTa1 (AAF00214), *S. fradiae* | 61/47 | Glycosyl transferase |
| *txnC4* | 240 | RedLA2 (AAT45284), *S. tubercidicus* | 82/73 | Ketoreductase |
| *txnM2* | 340 | MetLA2 (AAT45283), *S. tubercidicus* | 79/70 | O-methyltransferase |
| *txnU4* | 388 | PAI11_01900 (EHN12885), *Patulibacter* sp. I11 | 82/69 | Unknown |
| *txnB11* | 397 | Azi15 (ABY83154), *S. sahachiroi* | 63/50 | O-acyltransferase |
| *txnB12* | 427 | UrdGTa1 (AAF00214), *S. fradiae* | 61/47 | Glycosyl transferase |
| *txnM3* | 339 | DmpM (AFE08598), *Corallococcus coralloides* DSM 2259 | 62/45 | O-methyltransferase |
| *txnO12* | 407 | FosK (AEC13077), *S. pulveraceus* | 67/54 | Cytochrome P450 |
| *txnM4* | 340 | DmpM (AFE08598), *Corallococcus coralloides* DSM 2259 | 61/44 | O-methyltransferase |
| *txnU5* | 182 | RAM_06565 (AEK39805), *Amycolatopsis mediterranei* S699 | 75/64 | Unknown |
| *txnRg6* | 286 | SARP regulator (ACU39492), *Actinosynnema mirum* DSM 43827 | 53/40 | Regulator |

[a] Amino acid, [b] Similarity/Identity.

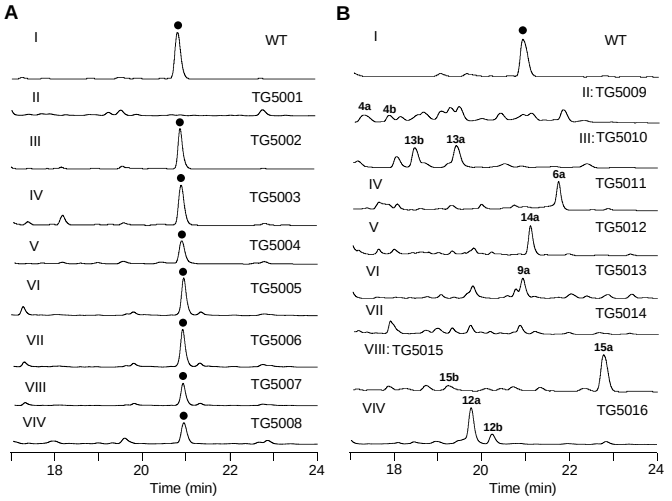


**Fig. 4** Genetic characterization of the genes for TXN biosynthesis *in vivo*. HPLC analysis of TXN-A and analogues production (UV at 271 nm) from *S. bottropensis*: I) wild-type NRRL 12051, A-II) mutant TG5001 (Δ*txn*A1), A-III) TG5002 (Δ*orf*-3), A-IV) TG5003 (Δ*orf*-1), A-V) TG5004 (Δ*txn*Rg1), A-VI) TG5005 (Δ*orf*+11), A-VII) TG5006 (Δ*orf*+3), A-VIII) TG5007 (Δ*txn*Rg6), A-VIV) TG5008 (Δ*txn*A4); B-II) TG5009 (Δ*txn*C2), B-III) TG5010 (Δ*txn*C4), B-IV) TG5011 (Δ*txn*C3), B-V) TG5012 (Δ*txn*O2), B-VI) TG5013 (Δ*txn*O5), B-VII) TG5014 (Δ*txn*O6), B-VIII) TG5015 (Δ*txn*O12), B-VIV) TG5016 (Δ*txn*B4). (●), TXN-A. The genotypes of all the mutants were confirmed by PCR analysis, and the results were summarized in Fig. S2.

**PKS and polyketide processing enzymes in TXN-A scaffold biosynthesis**

Bioinformatic analysis not only gives the expected minimal PKS encoded by *txn*A1 (KS), *txn*A2 (CLF), and *txn*A3 (acyl carrier protein, ACP), but also reveals a malonyl-CoA:ACP transacylase (MAT, *txn*A4) and a KS-III (*txn*A5), which are less frequently involved in the type-II PKS machinery.[13,15] The inactivation of *txn*A4 significantly reduced the production of TXN-A with 20%-30% to that of WT (Figure 4A-VIV). This phenomenon is reasonable, for the partially functional complementation by the MAT of fatty acid biosynthesis. Deeply analysis of CLF (TxnA2) revealed the gatekeeper residues as G113-L117-W195-V110-G196-M151-F134, which shows specificity toward the C-23 polyketide length.[16,17] Additionally, two genes (*txn*C2 and *txn*C4) encode enzymes bearing high sequence homology (60%-75% identity) with typical ketoreductases (KRs), while TxnC2 shows more closely to the C-9 KRs, which involved in the folding and cyclization of the nascent polyketide chain.[18,19] TxnC1 is relatively close to the aromatase likely responsible for the C7-C12 cyclization of the first ring followed the ketoreduction of C-9 by TxnC2, and TxnC3 shares high sequence similarity with 2,3-cyclase, which catalyzes the second and third cyclization steps to form the aromatic ring intermediate **7** (Fig. 3B).

To verify the hypothetical functions of the relative genes in TXN-A biosynthesis, *txn*C2, *txn*C3 and *txn*C4 were inactivated separately by gene replacement with the *aac(3)IV* apramycin-resistance gene (ESI, Fig. S2). The resultant mutant strains *S. bottropensis* TG5009 (Δ*txn*C2), TG5010 (Δ*txn*C4) and TG5011 (Δ*txn*C3) all abolished to produce TXN-A; whereas, each of the three mutants accumulated new compounds that are different from TXNs (Fig. 4B-II, III and IV). Following the optimized fermentation and isolation processes (including silica gel and Sephadex LH-20 column chromatography, preparative HPLC *et al*), we obtained 10 mg of **4a** and 6 mg of **4b** from an 8 L culture of TG5009 strain; 11 mg of **13a** and 2 mg of **13b** from a 4 L broth of TG5010 strain; as well as 40 mg of **6a** from a 2 L culture of TG5011 strain. The chemical structures of these compounds were elucidated by MS, HRMS and 1D-, 2D-NMR spectrum (Fig. S3-S17, S28-S32 and Table S4, S5, S8, S11) and summarized in Fig. 5. These results strongly supported the

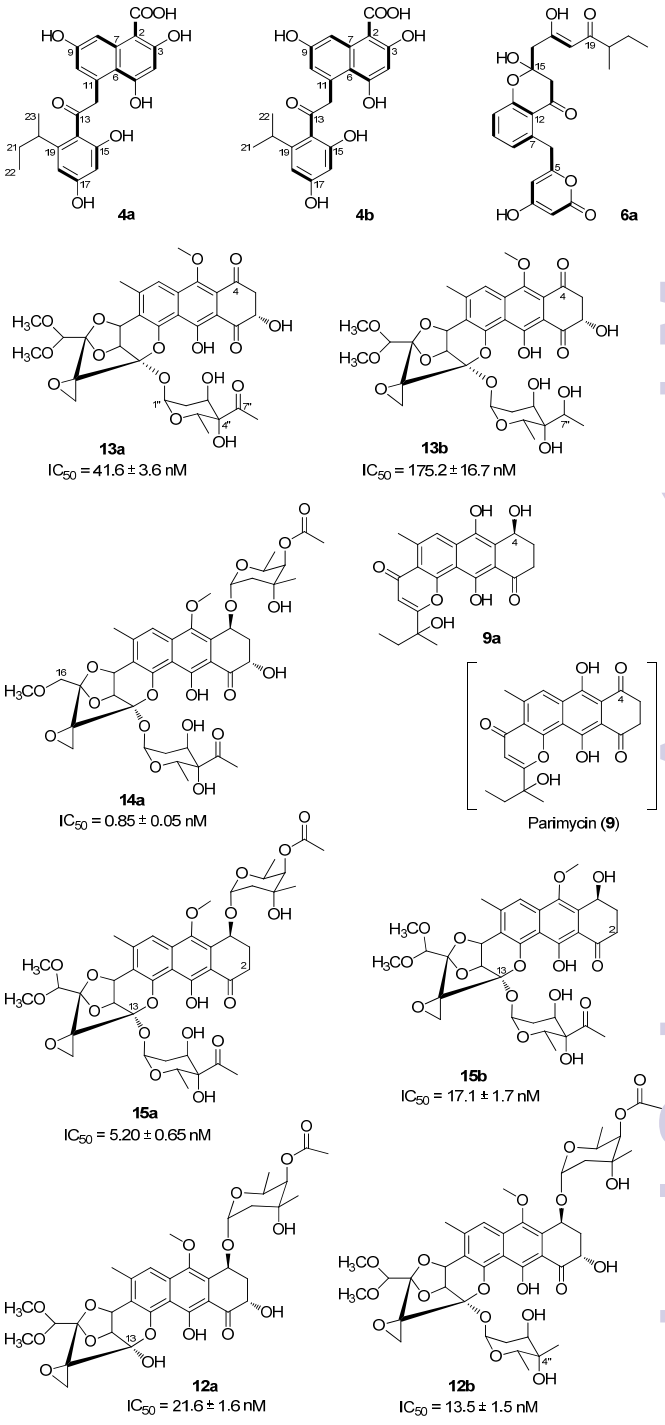


**Fig. 5** Chemical structures of the TXN-A analogues or relative metabolites produced by the mutants.

biological function of the respective gene and the proposed biosynthetic pathway (Fig. 3B). First, the production of compounds **4a** and **4b** by TG5009 (Δ*txn*C2) mutant verified that TxnC2 reduces the C-9 keto group of the nascent polyketide chain. More importantly, this result indicated that the reduction of C-9 is necessary for the next C7-C12 cyclization and aromatization, and similar opinion have been widely accepted in type II PKS.[19,20] Whereas, the production of a small amount of **4b** is unexpected but reasonable, which could be derived from the incorporation of *L*-valine through deamination and deacrboxylation similar to that of avermectin "b" components biosynthesis.[12,21] Second, the TG5011 (Δ*txn*C3) mutant affording compound **6a** double confirmed that TxnC2/C1 catalyze the C7-C12 first-ring cyclization and aromatization, and similar cyclized compound SEK4 had ever been generated by octaketide minimal PKS excepted with different starter unit and chain length.[19,22] Third, isolation **13a** and **13b** from TG5010 (Δ*txn*C4) mutant suggested that this KR catalyzes another ketoreduction, such as **10** into **11** (Fig. 3B), which afford the hydroxyl group for deoxysugar attachment. In collection, the two new compounds **4a** and **4b** further established that a different five-carbon starter unit for type-II PKS in TXN biosynthesis. Given the fact that the starter unit has been proved to be an attractive point for engineering aromatic polyketide biosynthetic machinery,[21,23] the discovery of different starter unit in TXN-A biosynthesis will also substantiates the potential of similar efforts.

In typically bacterial type II PKS system, a MAT sharing with fatty acid biosynthesis loads malonyl-CoA onto the thiol group of the 4'-phosphopantheinyl arm attached to the ACP, which is subsequently decarboxylated to generate an acetate starter unit and also used as extender units catalyzed by a KS-CLF heterodimer.[13,15] While, non-acetate starter units have been increasingly observed as alternative primers and usually involved an additional KS-III.[13] Based on the precursor feeding, bioinformatic analysis and genetic characterization results, we could propose that the biosynthetic pathway of the TXN-A polyketide backbone follows the action of a special type II PKS (TxnA1-A2-A3) as illustrated in Fig. 3B. The enzymes involved in the branched-chain fatty acids catabolism, a transaminase and a branched-chain 2-oxo acid dehydrogenase catalyze the deamination and deacrboxylation reactions to generate 2-methylbutyryl-CoA, which might be a direct starter unit for the KS of type II PKS primed by KS-III, TxnA5. Nine units of malonyl-CoA are subsequently incorporated into the PKS biosynthetic system by MAT (TxnA4) to form the full elongated polyketide chain **4**. Next, the PKS associated enzymes KR (TxnC2), aromatase (TxnC1), and cyclase (TxnC3) are required to carry out the regioselective folding and cyclization of the nascent chain to yield aromatic polycyclic backbone **7**. Subsequently, a decarboxylation and further cyclization steps should be involved to yield the intermediate **8**.

**Tailoring enzymes for further modifications in TXN-A scaffold biosynthesis**

The extremely complex structural features of TXN-A indicated that a large amount of unusual post-PKS modification steps should be involved to construct the framework. Indeed, the *txn* gene cluster encodes four methyltransferases (MTs, TxnM1-M4), twelve enzymes possibly relative to oxidation-reduction (TxnO1-O12), two hydrolases (TxnH1-H2), and nine proteins with unknown functions (TxnP1-P4, TxnU1-U5). Excepted the MTs, most taloring enzymes could not be easily assigned the physilogical roles in the biosynhthetic pathway.

Totally four cytochrome P450 enzymes (P450s) encoded by *txn*O2, O5, O6 and O12 attracted our attentions because this family of oxidative hemoproteins could catalyze a lot of different reactions for structural diversification in natural product biosynthesis.[24] Therefore, we constructed the respective gene replacement mutants *S. bottropensis* TG5012 (Δ*txn*O2), TG5013 (Δ*txn*O5), TG5014 (Δ*txn*O6) and TG5015 (Δ*txn*O12), and analyzed the metabolites production by HPLC and LC-MS. The results showed that each of the four mutants afforded compounds different from wild type (Fig. 4B-V to VIII). Although attempts to isolate new compounds from TG5014 (Δ*txn*O6) mutant were unsuccessful for the low yield and instability, we finally obtained 40 mg of **14a** from a 1 L culture of TG5012 strain, 15 mg of **9a** from a 4 L fermentation broth of TG5013 mutant, as well as 20 mg of **15a** and 4 mg of **15b** from a 2 L culture of TG5015 strain. Evaluation of MS, NMR spectra and comparison with TXN-A (Fig. S18-S21, S33-S44 and Table S6, S9-S11) led to successfully assign the chemical structures of all these new compounds (Fig. 5).

Structurally, compound **9a** is close to parimycin (**9**, Fig. 5) which was isolated from another TXN-A producing strain, marine *Streptomyces* sp. B8652, as a novel 2,3-dihydro-1,4-anthraquinone unrelated with TXNs.[25] The isolation **9a** from Δ*txn*O5 mutant not only hinted that this P450 plays a key role in the formation of the highly oxygenated polycyclic skeleton, but also suggested that **9** or **9a** should be the intermediate for the biogeneration of TXN-A (Fig. 3B). We believe that TxnO5 (P450), or/and TxnO6 (P450), TxnO4 (ferredoxin), TxnO3 (ferredoxin reductase), TxnH2 (epoxide hydrolase), and TxnM3 or M4 (MT) should be involved in the transformation of **10** from **9** (Fig. 3B and S45), while this complex process may need more uncharacterized enzymes. In addition, the production of **14a** by Δ*txn*O2 mutant and **15a**/**15b** by Δ*txn*O12 mutant showed that the P450s catalyze hydroxylation at C-16 and C-2 position, respectively.

**Deoxysugars pathway in TXN-A biosynthesis**

Glycosylation modifications of natural products are usually important diversification steps leading to the corresponding ultimate bioactive compounds.[26] TXN-A contains two deoxysugar moieties including a rare γ-branched octose with a two-carbon side chain attached at C-4'' position. Total thirteen genes (*txn*B1-*txn*B12 and *txn*M1) in *txn* gene cluster encoding enzymes are well consistent with the biosynthesis of two sugar moieties and subsequently attachment to the aglycon (Fig. 3C and 3B). A thymine diphosphate (dTDP)-glucose synthetase (TxnB2), a dTDP-glucose 4,6-dehydratase (TxnB1) and a dNDP-hexose 2,3-dehydratase (TxnB7) catalyze the generation of **16** from glucose-1-phosphate, which possibly served as the branch point for the biosynthesis of deoxysugar donors **19** and **22** (Fig. 3C). Sequentially acted by a 4-ketoreductase (TxnB5), a dTDP-hexose 3-C-MT (TxnM1), and a O-acyltransferase (TxnB11), the intermediate **16** could be converted into **22**, one deoxysugar donor for the formation of TXN-A (Fig. 3C). On the other hand, a 3-ketoreductase (TxnB8) and a 3,5-epimerase (TxnB6) would perform the generation of **18** from **16**, which could be further attached with a two-carbon side chain derived from pyruvate catalyzed by a two-component pyruvate dehydrogenase like enzymes (TxnB3/B4) to yield another deoxysugar donor **19** (Fig. 3C). A similar process was also proposed for the same deoxysugar moiety in the biosynthesis of kosinostatin,[14] yersiniose A,[27] and avilamycin A.[28] Finally, two deoxysuger donors **19** and **22** would be installed onto the TXN scaffold catalyzed by glycosyl transferases (TxnB9, TxnB10 or TxnB12) to afford the final product TXN-A.



 

To obtain further insight into the deoxysugars pathway, especially the usual γ-branched octose, we inactivated the *txn*B4 gene resulting the mutant strain *S. bottropensis* TG5016 (Δ*txn*B4). This mutation completely abolished TXN-A production but yielded two new compounds (Fig. 4B-VIV). After fermentation and purification, we isolated 10 mg of **12a** and 3 mg of **12b** from a 1 L culture, and the structures were shown in Fig. 5 (Fig. S22-S27 and Table S7, S11). Compared with TXN-A, the major compound **12a** lost the γ-branched octose moiety at 13-OH, it means that the respective glycosyl transferase bears relatively strict substrate specificity toward the two-carbon side chain. The production of the minor compound **12b** revealed that a sugar C-MT, most likely TxnM1, catalyzes a methylation reaction to form a new sugar donor **23**, which partially completed **19** to generate **12b**, though it is not the perfect sugar donor for the glycosyl transferase comparable to the native **19** (Fig. 3C, B).

**Bioactivity of TXN analogues and primary structure-activity relationship**

With seven TXN-A analogues in hand, we subsequently performed *in vitro* cytotoxicity assays of these compounds using cultured Jurkat cells. As a positive control, TXN-A shows high activity with $IC_{50}$ value of 0.78 ± 0.08 nM; and the $IC_{50}$ values of these analogues were also measured and listed below the respective structure in Fig. 5. The most potent compound **14a**, exhibits excellent activity having a $IC_{50}$ value of 0.85 ± 0.05 nM, which is comparable to that of TXN-A. Another promising compound **15a** ($IC_{50}$ = 5.20 ± 0.65 nM), which was also chemically synthesized by Myers's group,[9] suggested that the 2-OH group is changeable for further drug development. In addition, the cytotoxicity of TXN-A is higher than that of **12a** or **13a**, and **15a** is more active than **15b** revealed that either of two deoxysugar moieties is important for the anticancer activity. Another interesting conclusion could be drawn that the two-carbon side chain of γ-branched octose is important for biological activity of TXN-A, because **12b** is more than 10-fold less potent. What's more, the keto group at C-7'' of this octose side chain could also contribute to the anticancer activity, which was supported by the observation of further less potent of **13b** than that of **13a**.

## Conclusions

Currently, the bacterial aromatic polyketides generated by type II PKSs have been well studied.[13,15,29,30] However, the unusual structure of TXN-A distinguished it from others and indicated that an unique biosynthetic machinery, including a series of sophisticated modifications, should be involved in the pathway. Our feeding experiments and genetic characterization of *txn* gene cluster have now revealed a novel precursor pathway for type II PKS. In addition, the TXN biosynthesis system employs extremely complex tailoring modifications, which suggested a vast of enzymatic reactions need to be explored. These findings have expanded our understanding of type II PKSs and set the stage for further combinatorial biosynthesis to yield more analogues towards drug discovery.

## Acknowledgements

We thank the supporting grants from 973 (2013CB836900), NSFC (81202442 & 81373307), and STCSM (14XD1404500) Programs.

## Notes and references

1 F. Tomita, T. Tamaoki, M. Morimoto and K. Fujimoto, *J. Antibiot.*, 1981, **34**, 1519–1524.
2 T. Tamaoki, K. Shirahata, T. Iida and F. Tomita, *J. Antibiot.*, 1981, **34**, 1525–1530.
3 K. Fujimoto and M. Morimoto, *J. Antibiot.*, 1983, **36**, 1216–1221.
4 R. P. Maskey, M. Sevvana, I. Usón, E. Helmke and H. Laatsch, *Angew. Chem. Int. Ed.*, 2004, **43**, 1281–1283.
5 R. P. Maskey, E. Helmke, O. Kayser, F. H. Fiebig, A. Maier, A. Busche and H. Laatsch, *J. Antibiot.*, 2004, **57**, 771–779.
6 A. Fitzner, H. Frauendrof, H. Laatsch and U. Diederichsen, *Anal. Bioanal. Chem.*, 2008, **390**, 1139–1147.
7 R. Pfoh, H. Laatsch and G. M. Sheldrick, *Nucleic Acids Res.*, 2008, **36**, 3508–3514.
8 J. Švenda, N. Hill and A. G. Myers, *Proc. Natl. Acad. Sci. U.S.A.*, 2011, **108**, 6709–6714.
9 T. Magauer, D. J. Smaltz and A. G. Myers, *Nat. Chem.*, 2013, **5**, 886–893.
10 L.-H. Qi, M. Zhang, H.-X. Pan, X.-D. Chen and G.-L. Tang, *Chin. J. Org. Chem.*, 2014, **34**, 1376–1381.
11 R. A. Thomas, *ChemBioChem*, 2001, **2**, 612–627.
12 H. Ikeda and S. Ōmura, *Chem. Rev.*, 1997, **97**, 2591–2609.
13 C. Hertweck, A. Luzhetskyy, Y. Rebets and A. Bechthold, *Nat. Prod. Rep.*, 2007, **24**, 162–190.
14 H.-M. Ma, Q. Zhou, Y.-M. Tang, Z. Zhang, Y.-S. Chen, H.-Y. He, H.-X. Pan, M.-C. Tang, J.-F. Gao, S.-Y. Zhao, Y. Igarashi and G.-L. Tang, *Chem. Biol.*, 2013, **20**, 796–805.
15 A. Das and C. Khosla, *Acc. Chem. Res.*, 2009, **42**, 631–639.
16 Y. Tang, S.-C. Tsai and C. Khosla, *J. Am. Chem. Soc.*, 2003, **125**, 12708–12709.
17 A.T. Keatinge-Clay, D. A. Maltby, K. F. Medzihradszky, C. Khosla and R. M. Stroud, *Nat. Struct. Mol. Biol.*, 2004, **11**, 888–893.
18 G. Lackner, A. Schenk, Z. Xu, K. Reinhardt, Z. S. Yunt, J. Piel and C Hertweck, *J. Am. Chem. Soc.*, 2007, **129**, 9306–9312.
19 H. Zhou, Y. Li and Y. Tang, *Nat. Prod. Rep.*, 2010, **27**, 839–868.
20 Y. Shen, P. Yoon, T. W. Yu, H. G. Floss, D. A. Hopwood and B. S. Moore, *Proc. Natl. Acad. Sci. U.S.A.*, 1999, **96**, 3622–3627.
21 B. S. Moore and C. Hertweck, *Nat. Prod. Rep.*, 2002, **19**, 70–99.
22 H. Fu, S. Ebert-Khosla, D. A. Hopwood and C. Khosla, *J. Am. Chem. Soc.*, 1994, **116**, 4166–4170.
23 T. S. Lee, C. Khosla and Y. Tang, *J. Am. Chem. Soc.*, 2005, **127**, 12254–12262.
24 L. M. Podust and D. H. Sherman, *Nat. Prod. Rep.*, 2012, **29**, 1251–1266.
25 R. P. Maskey, E. Helmke, H.-H. Fiebig and H. Laatsch, *J. Antibiot.*, 2002, **55**, 1031–1035.
26 C. J. Thibodeaux, C. E. Melancon III and H.-W. Liu, *Angew. Chem. Int. Ed.*, 2008, **47**, 9814–9859.
27 H. Chen, Z. Guo and H.-W. Liu, *J. Am. Chem. Soc.*, 1998, **120**, 11796–11797.
28 I. Treede, G. Hauser, A. Mühlenweg, C. Hofmann, M. Schmidt, G. Weitnauer, S. Glaser and A. Bechthold, *Appl. Environ. Microbiol.*, 2005, **71**, 400–406.
29 M. Metsä-Ketelä, J. Niemi, P. Mäntsälä and G. Schneider, *Top. Curr. Chem.*, 2008, **282**, 101–140.
30 M. K. Kharel, P. Pahari, M. D. Shepherd, N. Tibrewal, S. Eric Nybo, K. A. Shaaban and J. Rohr, *Nat. Prod. Rep.*, 2012, **29**, 264–325.